Study of an ultrahigh-numerical-aperture fiber continuum generation source for optical coherence tomography

Daniel L. Marks, Amy L. Oldenburg, and J. Joshua Reynolds

Department of Electrical and Computer Engineering, Beckman Institute for Advanced Science and Technology, University of Illinois at Urbana–Champaign, 405 North Mathews Avenue, Urbana, Illinois 61801

Stephen A. Boppart

Department of Electrical and Computer Engineering, Bioengineering Program, Beckman Institute for Advanced Science and Technology, College of Medicine, University of Illinois at Urbana–Champaign, 405 North Mathews Avenue, Urbana, Illinois 61801

Received July 16, 2002

The axial resolution of optical coherence tomography images is primarily dependent on the bandwidth of the illumination source. Continuum generation is one way to generate the single-mode, high-bandwidth light needed for point illumination. We present an inexpensive and easy-to-implement augmentation to a Ti:sapphire laser that widens the bandwidth from 20 to over 200 nm with commerically available ultra-high-numerical-aperture fiber. This technique can provide a readily available broad-bandwidth source for researchers and a practical enhancement to a fiber-optic optical coherence tomography system.

OCIS codes: 190.7110, 110.4500, 190.4370.

Optical coherence tomography (OCT) requires an optical source of high bandwidth in a single spatial mode. Many researchers[1–5] have used ultrafast pulse generation and continuum generation[6,7] to create a better OCT source. However, often these sources use exotic custom-made optical components or specialized fibers that are not mass produced or readily available to researchers. We investigated methods to construct a source that was inexpensive and could be readily reproduced by our peers without fiber manufacturing facilities. A reproducible source might allow the entire OCT community to better compare results as well as realize the benefits of such research. We present a practical, easily obtainable alternative that can inexpensively increase the bandwidth of a 20-nm mode-locked Ti:sapphire source to over 200 nm and is easily integrated into a fiber-optic OCT setup. Furthermore, this technique produces a stable spectrum, which is essential for reproducible imaging. We utilize fiber with an ultrahigh numerical aperture (NA), which has a very narrow core and is suitable for concentrating light to enhance nonlinear processes. Three ultrahigh-NA fiber types are examined, with various excitation wavelengths and source bandwidths. Since nonlinear processes can be challenging to model, this information could be used for verifying these models.

Continuum generation in optical fiber has a number of practical difficulties that subsequently require that very specialized fibers be made. Typical single-mode fibers have a mode diameter of 5–10 μm and have normal dispersion in the near-infrared wavelengths. Since the nonlinear processes of continuum generation are sensitive to intensity, low peak intensity results in negligible bandwidth broadening of a pulse. In addition, dispersion induces temporal broadening of the pulse, further reducing the peak intensity. To combat these problems, researchers have used narrowly tapered fibers,[8] dispersion-shifted fibers,[9] and microstructured fibers.[4,10–12] Narrowly tapered fibers are stretched to 2–3-μm diameter so that the core of the fiber vanishes, and the air–glass boundary guides the pulse. The taper spatially concentrates the pulse and enhances the nonlinear effect. Microstructured fibers attempt to both confine the light spatially and alter the dispersion characteristics of the fiber. Although both narrowly tapered and microstructured fiber methods have been very effective, producing a broadband signal from 400 to 1500 nm, they are not readily available.

We investigated fibers with a narrow core that would act as a taper to enhance the nonlinear effect but would not be fragile or difficult to fabricate. Ultrahigh-NA fiber is a standard silica fiber with a nearly pure GeO_2 core. These fibers are manufactured by Nufern, and distributed by Thorlabs. A technical representative of the manufacturer claims that the index profile is similar to that of a step-index fiber but with proprietary methods of enhancing the NA. We tested three fiber types, UHNA1, UHNA3, and UHNA4, with NAs of 0.28, 0.35, and 0.35, second-mode cutoff wavelengths of 1000, 850, and 1050 nm, and mode field diameters (at 1100 nm) of 3.3, 2.5, and 2.6 μm, respectively. Based on these data and the assumption of a step-index fiber, it is possible to estimate the core GeO_2 concentration, but this was not necessary to utilize the fiber.

To excite the fibers we used a mode-locked Ti:sapphire laser (KMLabs, Boulder, Colo.) that produced ~400-mW output at a 90-MHz repetition rate, yielding 4.4-nJ pulses. We coupled the light into the fiber with a 0.5-NA, 1.5-mm-diameter aspheric lens. An aspheric lens was used rather than an achromat lens because the typical thick achromat lens itself can produce considerable dispersion, and the aspheric

0146-9592/02/222010-03$15.00/0

lens produces a small focal spot. So that they could be spliced with standard optical fiber, UHNA fibers have a diameter of 125 μm and therefore could be spliced onto standard fibers. However, the difference in mode diameters introduces great losses in power at the splice. We spliced these fibers onto Corning HI-780 and 3M FS-SN-4224 fiber, created for use at 800-nm wavelengths. We could typically couple 300–350 mW into the ultrahigh-NA fiber, and at least 70–100 mW of the light was conducted into the larger-core fiber in all cases. Although this loss is great, 70–100 mW of light is more than adequate for most OCT work, in which one usually limits the sample-illumination power to 10 mW to prevent sample damage. We noticed no problems resulting from utilizing the fibers at wavelengths below the second mode cutoff, probably because the second fiber acted as a spatial filter. The coupling between the fiber types produced little change in the spectrum.

Figure 1 shows the input and output spectra of all three fibers with two different excitation wavelengths. The length of each fiber was at least 1 m. A fiber-coupled spectrometer at the output of the ultrahigh-NA fiber measured the continuum spectrum. The achieved bandwidth was power and coupling dependent, so the spectra shown in Fig. 1 were optimized for maximum bandwidth. We found a strong tendency for the fibers to broaden the spectrum toward shorter wavelengths. As a result, pulses starting with longer wavelengths tended to produce wider bandwidth broadening. However, there seemed to be a limit at 670 nm below which the fibers would not produce any further broadening. Since the fibers are expected to be multimode at this wavelength, modal dispersion may disperse the pulse. Also, the GeO_2 core may absorb or scatter visible wavelengths. It was observed that a small amount of multiline argon-ion pump light from 476 to 514 nm, when it was coupled into the fibers, appeared greener at the output, suggesting increased attenuation of shorter wavelengths. These fibers, however, were not intended for use at visible wavelengths. The broadened non-Gaussian spectra generated by these ultrahigh-NA fibers, and similarly for tapered and microstructured fibers, will produce large sidelobes in the autocorrelation of these spectra. We calculated the ratio of the peak magnitude to the first-sidelobe magnitude in decibels for each of the spectra shown in Fig. 1. Without spectral reshaping or digital postprocessing of the data, the sidelobes produced by the supercontinuum spectra may somewhat obscure adjacent features.

It was observed that the UHNA3 fiber produced the greatest degree of broadening, in some cases achieving 250 nm of bandwidth from 700 to 950 nm. However, UHNA3 was also prone to producing non-Gaussian spectra. The spectrum was very sensitive to the coupling conditions and power. By adjusting them, we could minimize the nonuniformities in the spectrum. There seemed to be a strong tendency to produce light near the 700-nm wavelength. UHNA4 produced somewhat less broadening but more often in a Gaussian-like shape preferred by those who perform coherence imaging. UHNA1 was similar to UHNA4, except that it produced even less broadening. Because of its large bandwidth, we chose to concentrate on exploring the capabilities of UHNA3.

To determine the length of fiber needed to achieve the measured bandwidth, we started with a 1.4-m length of UHNA3 and measured the spectrum as the fiber was shortened. Figure 2 shows the spectra of the continuum generation for three different lengths. No significant degradation in bandwidth was detected for the shortest length used, 7.4 cm. However, as the spectrum is less uniform, longer lengths of fiber may help homogenize the spectrum. Testing shorter lengths was difficult because pump light coupled into the cladding overwhelmed the continuum signal. This short length suggests that most of the nonlinear spectral broadening occurs near the entrance facet of the fiber. It is likely that dispersion effects limit the length of fiber over which the peak pulse intensity is maintained. Also, the pulse is slightly chirped when it emerges from the Ti:sapphire laser, because the

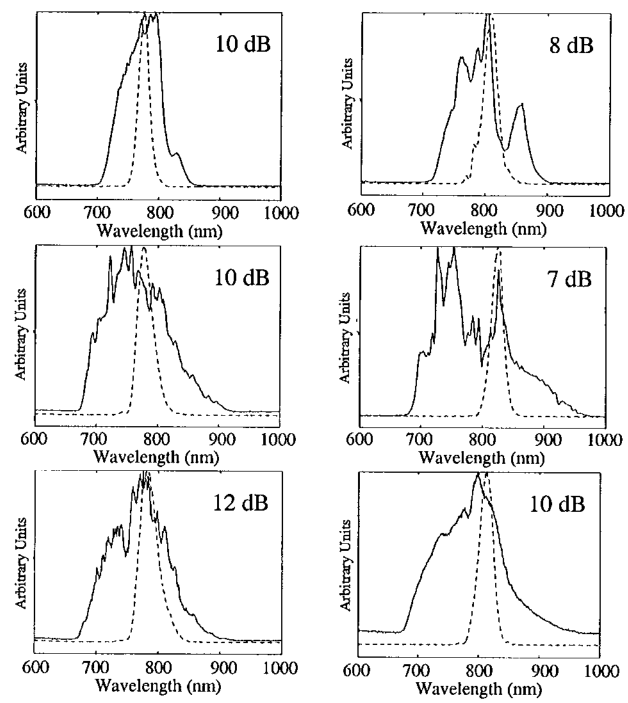

Fig. 1. Normalized spectra of UHNA fibers pumped with a Ti:sapphire laser at various center wavelengths and 10–20-nm bandwidth. The top two spectra are UHNA1, the middle two are UHNA3, and the bottom two are UHNA4. Dashed curves, original input spectra; solid curves, output spectra. All spectra are on a linear scale. The dB reading is the ratio of the magnitude of the main lobe to the first sidelobe of the point spread function.

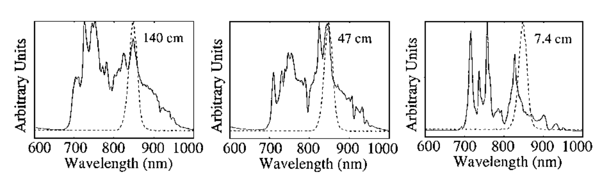

Fig. 2. Spectra of UHNA3 with various fiber lengths. Dashed curves, original input spectra; solid curves, output spectra.

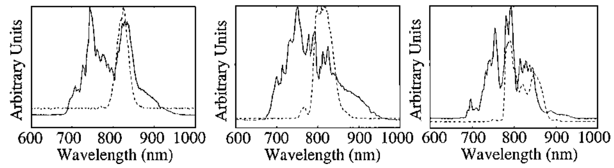

Fig. 3. Spectra of UHNA3 with different excitation bandwidths. Dotted curves, original input spectra; solid curves, output spectra.

pulse travels through the Ti:sapphire crystal before emerging from the output coupler. Utilizing a pair of dispersing prisms, we attempted to compensate for this slight chirping outside the cavity, but bandwidth improvement as a result of the pulse compression was not readily apparent. We did not know our exact pulse length, as we lacked an intensity autocorrelator.

We also explored the effect of the bandwidth of the pulse on continuum generation. Figure 3 shows the generated spectrum for several different input bandwidths. The bandwidths of the input pulse did not seem to influence the generated continuum bandwidth significantly. Since the output of the laser was slightly chirped, it may be that the peak intensity did not reach the magnitude needed to exploit the nonlinear effect fully. However, since large bandwidths seem to have the same broadening limitations as small bandwidths, it is likely that some other factor is limiting.

In practice it is known that nonlinear processes are power and pulse-length sensitive. In particular, continuum generation in these fibers is a combination of processes such as self-phase modulation, stimulated Raman scattering, and four-wave mixing, among others. Therefore, the output is very sensitive to the power, wavelength, bandwidth, and chirp of the input pulses. Fluctuations in the oscillator or changes in the fiber coupling could cause significant short- and long-term drift in the spectrum, introducing another noise source into coherence imaging. When utilizing ultrahigh-NA fiber, we found UHNA4 to produce a consistent low-noise spectrum that provided clear images, whereas UHNA3 was somewhat more sensitive to fluctuations and required that the oscillator be very stable. In general, we found that more spectral fluctuations occur as the bandwidth of the continuum widens. Nevertheless, we were able to produce OCT images with both fibers, albeit more reliably with UHNA4.

Although the ultimate bandwidth achievable with ultrahigh-NA fiber may be limited, we have demonstrated that using ultrahigh-NA fiber is a useful way to significantly broaden relatively low-bandwidth pulses from ultrafast lasers. Since 200 nm of bandwidth centered at 800 nm can potentially yield 1-μm resolution in tissue ($n = 1.4$), this technique represents a readily available and practical method for achieving the bandwidth needed to image biological structures at the cellular level. Further work will be needed to compensate for material dispersion, better optimize the bandwidth produced in the fiber, and minimize the sidelobes that occur because of any given generated spectral shape. Ultrahigh-NA fibers are a practical and useful technique with which to increase spectral bandwidth and axial resolution in a fiber-optic-based OCT system.

This research was supported by the National Science Foundation (grant BES-0086696), the Whitaker Foundation, the National Aeronautics and Space Administration (grant NAS2-02057), the National Cancer Institute, and the Beckman Institute. S. A. Boppart's e-mail address is boppart@uiuc.edu. D. L. Marks's e-mail address is dmarks@uiuc.edu.

References

1. D. Huang, E. A. Swanson, C. P. Lin, J. S. Schuman, W. G. Stinson, W. Chang, M. R. Hee, T. Flotte, K. Gregory, C. A. Puliafito, and J. G. Fujimoto, Science **254,** 1178 (1991).
2. B. E. Bouma and G. J. Tearney, eds., *Handbook of Optical Coherence Tomography* (Marcel Dekker, New York, 2001).
3. S. A. Boppart, B. E. Bouma, C. Pitris, J. F. Southern, M. E. Brezinski, and J. G. Fujimoto, Nature Med. **4,** 861 (1998).
4. I. Hartl, X. D. Li, C. Chudoba, J. G. Ko, T. H. Ko, J. G. Fujimoto, J. K. Ranka, and R. S. Windeler, Opt. Lett. **26,** 608 (2001).
5. W. Drexler, U. Morgner, F. X. Kärtner, C. Pitris, S. A. Boppart, X. Li, E. P. Ippen, and J. G. Fuijimoto, Opt. Lett. **24,** 1221 (1999).
6. R. R. Alfano, *The Supercontinuum Laser Source* (Springer-Verlag, New York, 1989).
7. G. P. Agarwal, *Nonlinear Fiber Optics* (Academic, San Diego, Calif., 2001).
8. T. A. Birks, W. J. Wadsworth, and P. St. J. Russell, Opt. Lett. **25,** 1415 (2000).
9. G. A. Nowak, J. Kim, and M. N. Islam, Appl. Opt. **38,** 7364 (1999).
10. S. Coen, A. H. L. Chau, R. Leonhardt, J. D. Harvey, J. C. Knight, W. J. Wadsworth, and P. St. J. Russell, J. Opt. Soc. Am. B **19,** 753 (2002).
11. J. M. Dudley, L. Provino, N. Grossard, H. Maillote, R. S. Windeler, B. J. Eggleton, and S. Coen, J. Opt. Soc. Am. B **19,** 765 (2002).
12. S. Coen, A. H. L. Chau, R. Leonhardt, J. D. Harvey, J. C. Knight, W. J. Wadsworth, and P. St. J. Russell, Opt. Lett. **26,** 1356 (2001).